Actin-Titin Interaction in Cardiac Myofibrils: Probing a Physiological Role

Wolfgang A. Linke,* Marc Ivemeyer,* Siegfried Labeit,# Horst Hinssen,§ J. Caspar Rüegg,* and Mathias Gautel#

*Institute of Physiology II, University of Heidelberg, D-69120 Heidelberg; #European Molecular Biology Laboratory, D-69012 Heidelberg; and §Biochemical Cell Biology Group, University of Bielefeld, D-33501 Bielefeld, Germany

ABSTRACT The high stiffness of relaxed cardiac myofibrils is explainable mainly by the expression of a short-length titin (connectin), the giant elastic protein of the vertebrate myofibrillar cytoskeleton. However, additional molecular features could account for this high stiffness, such as interaction between titin and actin, which has previously been reported in vitro. To probe this finding for a possible physiological significance, isolated myofibrils from rat heart were subjected to selective removal of actin filaments by a calcium-independent gelsolin fragment, and the "passive" stiffness of the specimens was recorded. Upon actin extraction, stiffness decreased by nearly 60%, and to a similar degree after high-salt extraction of thick filaments. Thus actin-titin association indeed contributes to the stiffness of resting cardiac muscle. To identify possible sites of association, we employed a combination of different techniques. Immunofluorescence microscopy revealed that actin extraction increased the extensibility of the previously stiff Z-disc-flanking titin region. Actin-titin interaction within this region was confirmed in in vitro cosedimentation assays, in which multimodule recombinant titin fragments were tested for their ability to interact with F-actin. By contrast, such assays showed no actin-titin-binding propensity for sarcomeric regions outside the Z-disc comb. Accordingly, the results of mechanical measurements demonstrated that competition with native titin by recombinant titin fragments from Z-disc-remote, I-band or A-band regions did not affect passive myofibril stiffness. These results indicate that it is actin-titin association near the Z-disc, but not along the remainder of the sarcomere, that helps to anchor the titin molecule at its N-terminus and maintain a high stiffness of the relaxed cardiac myofibril.

INTRODUCTION

Nonactivated preparations of cardiac muscle have long been known to be much stiffer than those of skeletal muscle. Earlier it was thought that the stiff "passive" elements of cardiac muscle are located outside the cell (e.g., Brady, 1968), but today it is clear that the high stiffness of cardiac preparations arises, at least partially, from structures within the myocyte (Fabiato and Fabiato, 1976; Brady, 1991; Granzier and Irving, 1995). Moreover, it has been demonstrated that already at the level of a single myofibril, cardiac specimens differ significantly from skeletal specimens in their passive mechanical properties, with the cardiac myofibrils being approximately an order of magnitude stiffer than the skeletal myofibrils (Bartoo et al., 1993; Linke et al., 1994, 1996b). These stiffness differences have been proposed to be due to the expression of different molecular size variants of titin (also called connectin; Wang et al., 1991; Horowits, 1992; Granzier and Wang, 1993), the giant elastic protein primarily responsible for the passive mechanical properties of vertebrate striated muscle (Maruyama et al., 1977; Wang et al., 1979; Horowits et al., 1986). The titin filaments, which span half-sarcomeres from the Z-disc to the M-line, are functionally stiff along their A-band portion, whereas they are elastic in the I-band (Fürst et al., 1988; Itoh et al., 1988; Trombitas and Pollack, 1993). It is within this I-band titin segment that most of the differential splicing occurs, with the consequence of cardiac titin having a much shorter elastic segment than skeletal titins (Labeit and Kolmerer, 1995a).

Although the expression of different length variants of I-band titin in various muscle types can potentially explain the stiffness differences between cardiac and skeletal fibers (for recent reviews, see Wang, 1996; Labeit et al., 1997), other mechanisms may also contribute to the high stiffness of cardiac myofibrils. Most notably, such mechanisms could include association of titin molecules with one another or with other sarcomeric proteins, particularly actin. Evidence has been found that actin and titin can interact in vitro (e.g., Maruyama et al., 1987; Soteriou et al., 1993; Jin, 1995). However, the physiological significance of this finding has remained unknown.

The present study was initiated to probe the titin-actin interaction reported in vitro for possible physiological relevance. We used a multifaceted approach, combining myofibril mechanics, immunofluorescence microscopy, and biochemical methods, to test whether the mechanical properties of cardiac muscle may be affected by actin binding to titin. We found that in the Z-disc comb, titin indeed associates with actin. Such an interaction will stiffen this region, thereby preventing slippage of the Z-disc titin segment during imposed stresses and hence contribute to a high passive stiffness of the sarcomere in vivo. Along the remainder of the sarcomere, we did not find evidence for actin-titin association, in the I-bands or in the A-bands. Thus the previously reported in vitro actin-titin interaction appears to be a factor in determining the mechanical properties of relaxed cardiac myofibrils only near the Z-disc.

Received for publication 31 October 1996 and in final form 17 April 1997.

Address reprint requests to Dr. Wolfgang A. Linke, Institute of Physiology II, University of Heidelberg, Im Neuenheimer Feld 326, D-69120 Heidelberg, Germany. Tel.: ++49-6221-544147; Fax: ++49-6221-544049; E-mail: wolfgang.linke@urz.uni-heidelberg.de.

0006-3495/97/08/905/15 $2.00

MATERIALS AND METHODS

Myofibril preparation and solutions

To prepare single cardiac myofibrils and small bundles of myofibrils, hearts from male Wistar rats were perfused at 4°C with rigor I solution containing 132 mM NaCl, 5 mM KCl, 7 mM glucose, 1 mM $MgCl_2$, 4 mM *N*-tris-(hydroxymethyl)methyl-2-aminoethanesulfonic acid, 5 mM EGTA, and 40 μg/ml leupeptin or one tablet of complete protease inhibitor cocktail tablets (Boehringer Mannheim, no. 1697 498) per 50-ml solution, pH 7.1 (adjusted with KOH), and right ventricles were dissected into thin strips. These were tied to thin glass rods and, for immediate use, skinned in rigor II solution (75 mM KCl, 10 mM Tris, 2 mM Mg Cl_2, 2 mM EGTA, protease inhibitors as above, pH 7.1, adjusted with KOH) containing 0.5–1% Triton X-100 for up to 4 h. Some muscle strips were also stored in rigor II/glycerol (50:50, v/v) solution at −20°C and were used within 2 weeks. To obtain single myofibrils, the skinned strips were minced and homogenized in rigor II (blender, Ultra-Turrax) at 4°C. From the suspension of myofibrils, a drop was placed in the specimen chamber (capacity, 200–300 μl), and myofibrils were allowed to settle. Then a single myofibril (or, when desired, a small myofibril bundle no wider than 6 μm) was selected for the experiment. All other solutions used, such as relaxing and activating solutions, were composed according to a solution component mixing protocol by Fabiato and Fabiato (1979) and had an ionic strength of 200 mM in a 3-(*N*-morpholino)propanesulfonic acid buffer, pH 7.1. Components included 4 mM Na_2ATP, 6 mM total magnesium, 15 mM EGTA, methane sulfonate as the major anion, and protease inhibitors as described above (Linke et al., 1994). Experiments were performed at room temperature.

Sodium dodecyl sulfate-polyacrylamide gel electrophoresis

Sodium dodecyl sulfate-polyacrylamide gel electrophoresis (SDS-PAGE) (Laemmli, 1970) was employed to investigate the protein composition of cardiac myofibrils in suspension. For the detection of smaller-molecular-weight proteins, we used 12% SDS gels, whereas for the dectection of titin, we used agarose-strengthened 2% polyacrylamide gels with a Laemmli buffer system (Tatsumi and Hattori, 1995). Care was taken to perform the specimen preparation procedure (including centrifugation) before solubilization in SDS buffer at 4°C, to avoid degradation of titin. Homogenized and repeatedly centrifuged tissue was dissolved in a buffer containing 1% SDS, 4 M urea, 15% glycerol, complete protease inhibitor cocktail tablets (Boehringer Mannheim) (one tablet per 50-ml solution), and 50 mM Tris-HCl, pH 6.8. The samples were then heated briefly to 95°C and separated on a minigel system (Bio-Rad). Protein bands were visualized with Coomassie brilliant blue R.

Preparation of gelsolin fragment

Gelsolin was prepared from pig stomach smooth muscle and purified as described previously (Hinssen et al., 1984). Purity of the preparations was monitored by SDS-PAGE (Laemmli, 1970), and protein concentration was determined by the microbiuret method (Goa, 1953). The calcium-independent N-terminal half of gelsolin (TL-40, M_r ~40 kDa) was prepared by proteolytic digestion of gelsolin with thermolysin (1:200 w/w, 25°C, 60 s) according to the method of Hellweg et al. (1993). The fragment was purified by anion exchange chromatography on Mono Q (Pharmacia) and stored in small units (concentration, 0.6–0.9 mg/ml) in a buffer containing 50 mM KCl, 1 mM $MgCl_2$, 1 mM EGTA, 20 mM imidazole, pH 7.2 at −80°C. Before an experiment, a unit was thawed and gelsolin was added to the relaxing solution to obtain a final concentration of at least 0.1 mg/ml.

Force/stiffness measurements

The setup used for passive tension/stiffness recordings is centered around a Zeiss Axiovert 135 inverted microscope equipped with phase-contrast optics (cf. Linke et al., 1993). The specimen is picked up with two glass microneedles, which are coated at their tips with a water-curing silicone adhesive in a 1:1 (v/v) mixture of Dow Corning 3145 RTV and 3140 RTV, to firmly anchor the myofibril ends. Both needles can be controlled by hydraulic micromanipulators (Narishige, Japan). One of the glass needles is attached to a piezoelectric micromotor, the other to a sensitive force transducer (both are home-built devices). The transducer, which operates on the basis of optical fiber beams, has a sensitivity of ~10 nN, at a resonant frequency of 700 Hz in water (Fearn et al., 1993). The myofibril image can be recorded by using either a 512-element linear photodiode array (Reticon Electronics) or a CCD video camera (FK440; Völker, Maintal, Germany), a video recorder (Panasonic NV-SD45), and/or a frame grabber board (Vision-EZ; Data Translation). Data collection is done with a 586 PC, a National Instruments data aquisition board (AT-MIO-16-F5), and LABVIEW software (National Instruments).

Steady-state passive force was measured as described previously by performing stretch-release cycles, interrupted by 2–3-min-long hold periods to allow for stress relaxation (Linke et al., 1996a). Force was expressed in units of mN/mm^2, with an approximation of the myofibril's cross-sectional area as in Linke et al. (1994) (precision of specimen edge detection, approximately ±0.2 μm). Dynamic stiffness was estimated from the amplitude of force response to 10–30 nm per half-sarcomere, peak-to-peak, sinusoidal oscillations (10–20 Hz) imposed by the motor. The oscillations were usually imposed for a duration of 2–4 s. The amplitude of sinusoidal length change was measured at the motor needle end, using either the CCD camera or the linear CCD array, and the average length change per half-sarcomere was deduced by assuming a similar change in each half-sarcomere. Obvious effects of possible myofibril end compliance (Friedman and Goldman, 1996) on the magnitude of length change per sarcomere were not detectable. Force values were recorded continuously in the course of an experiment at intervals of 4 ms and were stored in spreadsheet or binary format for later analysis. Before being considered for the stiffness calculations, the raw data were filtered off-line with a Butterworth bandpass filter (cf. Fig. 3 *A*). From the filtered data, stiffness was calculated by averaging the peak-to-peak amplitude of 20–30 force oscillations and was normally expressed as relative stiffness (percentage of control, relaxed, stiffness).

Because we used low-frequency sinusoids, we assumed that the entire myofibril stiffness measured was due to the presence of "passive" elastic filaments (principally titin) and excluded a possible contribution from viscoelastic, weakly bound cross-bridges (Kraft et al., 1995) or viscous elements within the actin-myosin overlap zone. This assumption was tested in control experiments, in which we analyzed the frequency dependence of relaxed myofibril stiffness, both before and after actin extraction by gelsolin. As shown in Fig. 1, we generally detected no frequency dependence of myofibril stiffness between 1 and 25 Hz. Above this frequency, however, we measured a steady stiffness increase in the control myofibrils. After actin extraction, which decreased stiffness by nearly 60% (cf. Results), we observed a frequency-dependent stiffness increase only above 100 Hz. Thus, just as desired, the low-frequency sinusoids of 10–20 Hz used in this study appear to be ineffective in detecting a possible stiffness contribution from weak cross-bridges or purely viscous elements.

Fluorescence microscopy

Actin filaments were visualized in an inverted microscope (epifluorescence modus, 100× oil immersion objective) with rhodamine-labeled phalloidin (no. P1951; Sigma) in a concentration of 0.5 μg/ml relaxing solution. For documentation, the myofibril image was photographed from the camera port of the microscope, using a Ricoh KR10M camera. The exposure time was 3–5 s.

Anti-titin immunofluorescence measurements were made for both relaxed (control) and actin-extracted myofibrils. Two alternative experimental protocols were used. In the first, a single myofibril was stretched slowly (~10% of its initial length per minute) from slack sarcomere length (SL) to a desired SL and was then repeatedly subjected to 2–3-s-long bursts of sinusoidal oscillations of the type imposed during stiffness measurements.

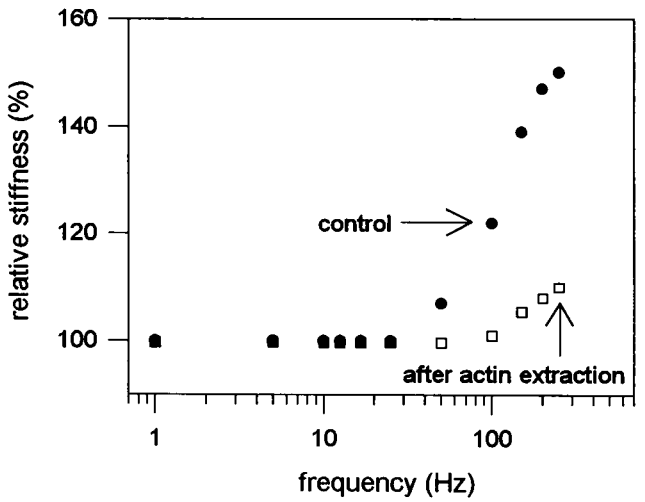

FIGURE 1 Frequency dependence of relaxed cardiac myofibril stiffness. Stiffness was measured from the force response of a 2.5-μm-thick myofibril bundle to small-magnitude sinusoidal oscillations at frequencies between 1 and 250 Hz. Stiffness was expressed in relative units, where 100% means stiffness at 1 Hz. Although not apparent in the figure, actin extraction by gelsolin fragment induced a substantial stiffness decrease, also at the lower frequencies (cf., Fig. 3). Note, therefore, that 100% stiffness refers to the 1-Hz stiffness of either control preparations (●) or actin-extracted myofibrils (□).

The specimen was then labeled with the monoclonal titin antibody T12 (kindly provided by D. O. Fürst; cf. Fürst et al., 1988) and, after washout, was secondary-labeled with tetramethylrhodamine isothiocyanate (TRITC)-conjugated anti-mouse IgG (whole molecule, no. T-5393; Sigma). The primary and secondary antibodies were normally used in dilutions of 1:50 (in relaxing solution); the exposure time to myofibrils was 20–30 min. Antibody epitope position was recorded by using the CCD video camera, frame grabber board, and image aquisition software (GlobalLab Aquire, Data Translation). In a second experimental protocol, the myofibril was first labeled with the T12 antibody and the fluorophore at slack SL and then stretched to a series of SLs, while the specimen was repeatedly exposed to brief bursts of sinusoidal oscillations, before an image was recorded. Both measurement protocols gave comparable results. As a control, we labeled myofibrils with the secondary antibody only, and found no fluorescence. Care was taken to expose the myofibril only briefly (<1 s) to the excitation light at any time of recording, to reduce the effect of photobleaching. At a given SL, we recorded two or three fluorescence images, which were then superimposed to increase resolution. With image analysis software (GlobalLab Image, Data Translation), the distance between two fluorescent antibody epitopes could be measured with a precision of approximately ±80 nm (cf. Fig. 6 *B*). Only regularly shaped fluorescence bands, the maximum fluorescence intensities of which differed by less than 20% from one another, were considered for those measurements.

Preparation of recombinant titin fragments

Recombinant cardiac titin fragments were cloned into a modified pET-vector, expressed solubly in BL21[DE3]pLysS, and purified as described previously (Politou et al., 1994; Freiburg and Gautel, 1996). Domain boundaries in the human cardiac titin peptide sequence (translated from X90568) were 1791–2126 (for the Z10/I1 construct), 4241–4697 (for I18/I20, harboring the whole cardiac PEVK segment), 5010–5507 (S53/S56 from X90569, for the N2-titin construct), 5237–5591 (for I27/I30), 5237–5959 (for I27/I34), 7170–7869 (I48/I54, for the $(FN3)_6$ construct), and 14255–14644 (for A65/A68). The fragment, Z10/I1, was expressed in Bl21[DE3] harboring the plasmid pUBS520 (Brinkmann et al., 1989). Constructs containing fibronectin (FN3) domains were chosen to have Ig-I domains at either end, because the N-terminal phasing of these domains is well characterized and crucial for a folded and, thus, functional domain (Politou et al., 1994). Proteins were dialyzed to F-buffer (see below) without calcium or EGTA and stored in this buffer at 4°C.

A65/A68 was also labeled with TRITC essentially as described (Harlow and Lane, 1988). Briefly, A65/A68 (1 mg/ml in 50 mM sodium phosphate, pH 8) was incubated at a molar ratio of 1:2 with TRITC for 30 min on ice. Unincorporated dye was separated by gel filtration on a NAP10 column (Pharmacia), equilibrated in relaxing buffer (cf. Myofibril preparation and solutions), and concentrated in a centricon ultrafiltration device (Filtron). Protein concentration was determined using the BCA kit (Pierce).

Circular dichroism

CD spectra in the far ultraviolet were recorded from the titin construct, I27/I30, in rigor II buffer. A Jasco J-710 spectropolarimeter was used, fitted with a thermostatted cell holder connected to a Neslab RTE-110 water bath. For further details, see Politou et al. (1995).

Actin-titin binding assay

G-actin and the recombinant titin fragments were incubated in 100 μl F-actin buffer (50 mM Tris/Cl, pH 8, 100 mM NaCl, 1 mM ATP, 1 mM dithiothreitol, 1 mM NaN_3), with either 0.1 mM $CaCl_2$ or 1 mM EGTA at 4°C, and with 20 μM actin and 5–50 μM titin fragments. After incubation for 30 min at 4°C, the F-actin was pelleted in a Beckman airfuge at 28 psi for 25 min, the supernatant was separated, and the pellet was dissolved in 100 μl of 4 M urea. After the addition of 100 μl sample buffer (Laemmli, 1970), samples were heated to 95°C for 3 min. For analysis, 5–10 μl of the sample was separated on 15% SDS-PAGE gels.

For visualization of the titin fragments Z10/I1 and I27/I30, Western blot analysis using the anti-His tag monoclonal antibody 13/45/31 (Dianova) was employed, because actin and some of the titin fragments studied were of similar size. Detection of bound antibody was performed with the ECL kit (Amersham).

Titin competition experiments

The effect of competitive titin binding to actin on myofibril stiffness was investigated in "competition assays," by using a variety of recombinant titin fragments. These included the I-band tandem-Ig module fragments I27/I30 and I27/I34, a four-Ig-domain fragment from the N2-titin segment, a six-domain FN3 construct from the edge of the A-band, and an A-band construct comprising the Ig/FN3 modules A65/A68 (cf. Fig. 7).

In a typical experimental protocol, a myofibril bundle no more than 4 μm thick (containing fewer than 10 myofibrils) was stretched in relaxing solution to an SL of 2.3–2.6 μm and was held at this SL for several minutes to allow for stress relaxation, and the stiffness of the specimen was measured from the force response to imposed sinusoidal oscillations as described above (cf. Force/stiffness measurements). Then successively increasing concentrations of recombinant titin fragments (0.04–15 mg/ml) were applied in relaxing solution while the stiffness was recorded. At a given fragment concentration, data from two to five stiffness measurements were averaged to increase resolution. The maximum experimental error was ±5%.

RESULTS

Passive tension/stiffness-sarcomere length curves

In an earlier study, it was shown that in relaxed, single myofibrils from rabbit heart, the shape of the sarcomere

length (SL)-passive tension curve is similar to that of the SL-passive stiffness curve, recorded from the force response to 500-Hz sinusoidal oscillations (Linke et al., 1996a). In the present study, we confirmed the similarity of the two curve types, also in relaxed, isolated myofibrils from rat heart exposed to low-frequency sinusoids of 10–20 Hz. We found that with a stretch from ~2.0 to ~3.0 μm SL, both passive tension and stiffness increase steadily (Fig. 2). Such a tension/stiffness increase has been suggested to result from the straightening of I-band titin domains during small stretches (up to an SL of 2.1–2.2 μm) and from the extension of individual titin domains at moderate to large degrees of stretch (up to an SL of ~3.0 μm; cf. Granzier et al., 1996; Linke et al., 1996a; Gautel et al., 1996b). Beginning at ~3.0 μm SL, the slope of the passive tension curve becomes greatly reduced, whereas the stiffness curve becomes flat (strain limit or "yield point"; Wang et al., 1991). Such curve flattening at extreme SLs is due to the release of previously bound A-band titin into the I-band, which affects the stiffness of the sarcomere (Wang et al., 1993; Linke et al., 1996a). In sum, the shape of both the SL-passive force and the SL-stiffness curve of single myofibrils appears to reflect the extension behavior of titin filaments during stretch. With the two curve types exhibiting a similar shape, we opted for measuring passive stiffness rather than steady-state passive tension in most experiments, because reproducibility of the stiffness data at comparable experimental conditions was excellent and independent of a slight force transducer baseline drift observed in some experiments.

Cardiac myofibril stiffness is reduced after selective actin extraction

To search for possible titin-actin interactions in cardiac muscle sarcomeres, we first tried to determine whether the passive stiffness of cardiac myofibrils may be affected by the removal of actin filaments. To depolymerize actin, we used the N-terminal half of gelsolin (TL-40), prepared by proteolytic digestion of purified gelsolin. TL-40 effectively severs F-actin in the absence of calcium ions (Hellweg et al., 1993; see also Granzier and Wang, 1993). The addition of a 0.1 mg/ml gelsolin fragment to the relaxing solution resulted in a marked decrease in myofibril stiffness (Fig. 3 *A*), usually within the first 1–3 min of application. Although not shown in Fig. 3 *A*, actin extraction also decreased steady-state passive tension in parallel with stiffness. This stiffness decrease was SL-dependent, with an average of 57 ± 10% (mean ± SD; $n = 13$) at SLs between 2.2 and 2.6 μm, but with a progressively smaller magnitude at longer lengths (Fig. 3 *B*). Above ~3.4 μm SL (i.e., above the strain limit in cardiac myofibrils; Trombitas et al., 1995; Linke et al., 1996a) the stiffness change was almost zero.

To test whether the stiffness decrease could result from the dissociation of residual actin-myosin cross-bridges present even under relaxing conditions, we carried out control experiments (Fig. 4 *A*). Because the addition of BDM (40–50 mM), a potent inhibitor of active force (e.g., Brotto et al., 1995), to the relaxing solution did not significantly

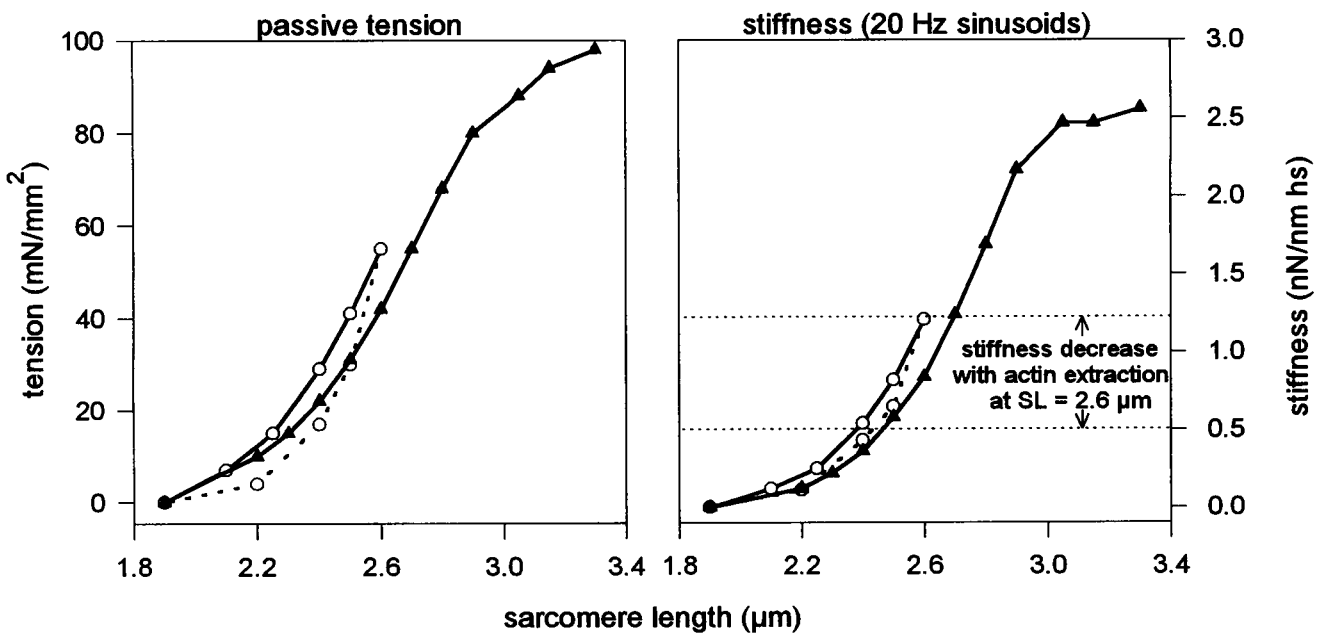

FIGURE 2 Passive tension-sarcomere length (SL) curve (*left*) and stiffness-SL curve (*right*) of a relaxed specimen consisting of two cardiac myofibrils. First the specimen was stretched in steps from slack SL to 2.6-μm SL, and released again. Then the preparation was extended beyond the strain limit (i.e., above ~3 μm SL), as indicated by a flattening of the curves. In this experiment, the stiffness values at a given SL (in units of nN per nm peak-to-peak oscillation amplitude per half-sarcomere) are lower than those in Linke et al. (1996a), which is mainly a result of the frequency dependence of myofibril stiffness (cf., Fig. 1); here we used low-frequency sinusoids to measure stiffness, whereas in the previous study, higher-frequency sinusoids of mostly 500 Hz were applied. For comparison, the approximate amount of stiffness decrease upon actin extraction at an SL of 2.6 μm (as reported in Fig. 3 *B*) is indicated by the dotted lines in the right panel. ——, Stretch; – – –, release; ○, first stretch-release cycle; ▲, second stretch.

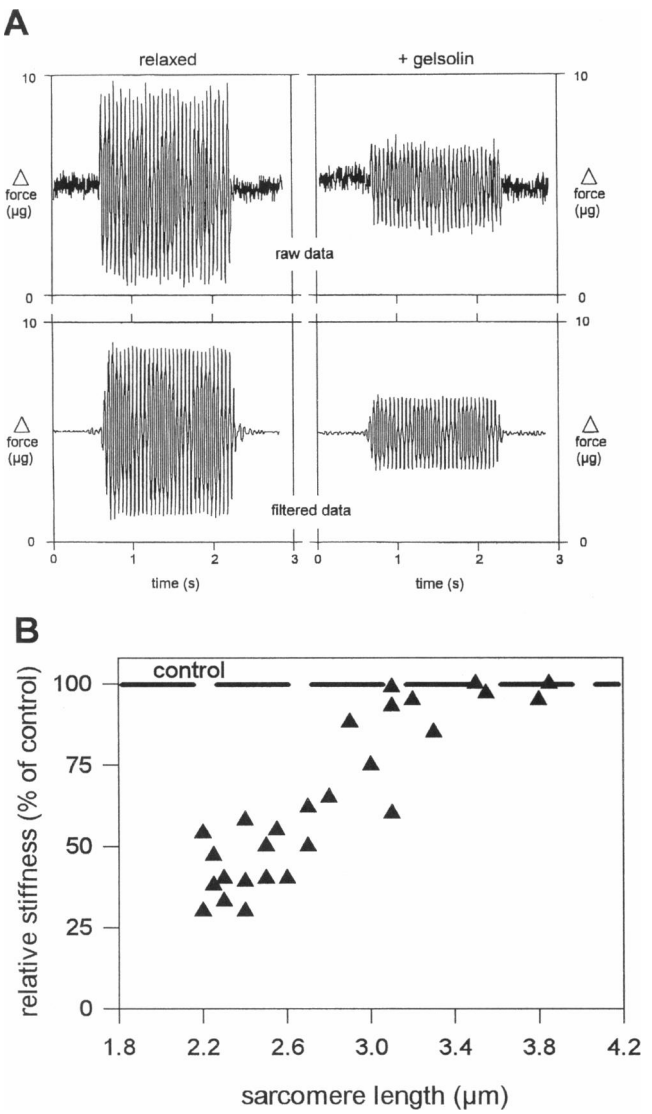

FIGURE 3 Actin extraction by gelsolin fragment reduces relaxed myofibril stiffness. (*A*) Representative force recordings (at 20-Hz sinusoidal frequency) from a 3-μm-thick myofibril bundle at SL = 2.4 μm, before (*left*) and after (*right*) actin extraction. The upper panels show original data; the data in the lower panels were obtained after filtering with a Butterworth bandpass filter. Sinusoidal force amplitude (representing stiffness) dropped by 58% during the extraction procedure (the stiffness change was calculated from the filtered data). (*B*) Summary of results of all measurements between 2.2 and 3.8 μm SL. "control" refers to the reference stiffness for each recording; the actual data points would be lined up along the dashed line (100% stiffness), but are not shown, for clarity.

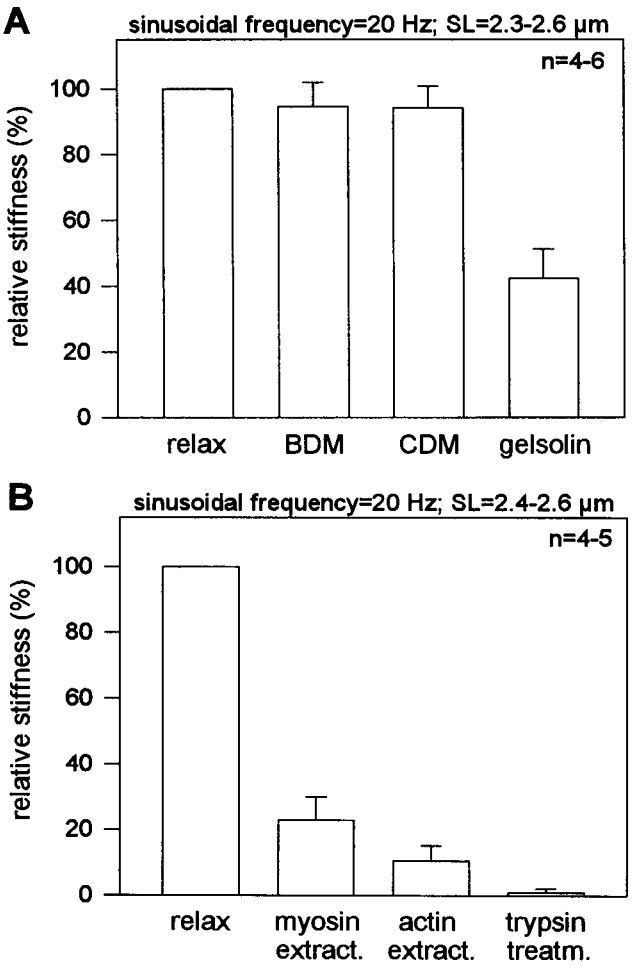

FIGURE 4 Controls to study a possible contribution of actomyosin cross-bridges to relaxed stiffness. (*A*) Effect of BDM (40 mM) and caldesmon (CDM, concentration, 0.35 mg/ml) in relaxing solution on myofibril stiffness. No statistically significant (Student's *t*-test) stiffness change was found with both substances, although in some experiments, application of BDM appeared to lower stiffness slightly. Treatment with gelsolin fragment (0.1 mg/ml), on the other hand, decreased stiffness greatly. (*B*) Effect of thick and thin filament removal on relaxed myofibril stiffness. In ~0.4 M KCl solution to extract thick filaments, stiffness decreased on average by 77%, whereas subsequent actin extraction lowered the stiffness by an additional 12%. Also shown, for comparison, is the effect of a 20-min-long mild trypsin treatment (final concentration, 0.25 μg/ml) on myofibril stiffness at the end of the extraction protocol. Stiffness approached zero, likely because of degradation of the titin filaments.

change the stiffness of cardiac myofibrils, we concluded that residual force-generating interactions did not appear to be a factor. Similarly, the possibility of weakly bound cross-bridges contributing to myofibril stiffness (Brenner et al., 1986) could be excluded, because caldesmon (concentration 0.35 mg/ml), which has been shown to prevent formation of weak cross-bridge states in striated muscle (Chalovich et al., 1991), did not affect relaxed myofibril stiffness (Fig. 4 *A*). The latter finding could be readily expected, because we used low-frequency oscillations and not the high-speed stretches or fast oscillations employed to detect possible weak bridge stiffness (cf. Fig. 1). In conclusion, the inhibition of residual actin-myosin interactions did not appear to be responsible for the gelsolin-induced stiffness decrease.

In addition, we tried to determine whether the stiffness decrease upon actin removal would still be evident after high-salt extraction of thick filaments (Fig. 4 *B*). We found that with the application of a drop of 400 mM KCl to the relaxing solution, the regular sarcomeric striation pattern was rapidly lost, and myofibril stiffness decreased within a

few seconds to 23 ± 7% (mean ± SD; $n = 5$; SL = 2.4–2.6 μm) of the control value, in agreement with previous reports by others (e.g., Roos and Brady, 1989). Such a stiffness decrease apparently results from the dissociation of A-band titin-thick filament bonds and hence, from an increase in the contour length of the elastic titin segment (Higuchi et al., 1992). When actin filaments were now selectively extracted by the application of a gelsolin fragment, stiffness decreased further to ~11% of the control value or by an additional 52 ± 5% (mean ± SD; $n = 4$; SL = 2.4–2.6 μm). With such a substantial decrease occurring in the myosin-depleted sarcomere, we concluded that the stiffness change upon gelsolin treatment is unrelated to structural changes within the A-bands.

Quality of actin extraction

The amount of stiffness decrease upon gelsolin treatment varied substantially between experiments, even at a given SL (cf. Fig. 3 *B*). We therefore tested whether such variability might be caused by incomplete removal of actin in some experiments. Actin extraction was investigated in the fluorescence microscope after each mechanical experiment, by using rhodamine-phalloidin as an actin marker. We generally found that in both single myofibrils and small bundles of myofibrils, actin removal was complete, except for a narrow region corresponding to the Z-discs (Fig. 5 *A*). In addition, actin extraction was also examined by SDS-PAGE on suspensions of cardiac myofibrils. In 12% gels, we found

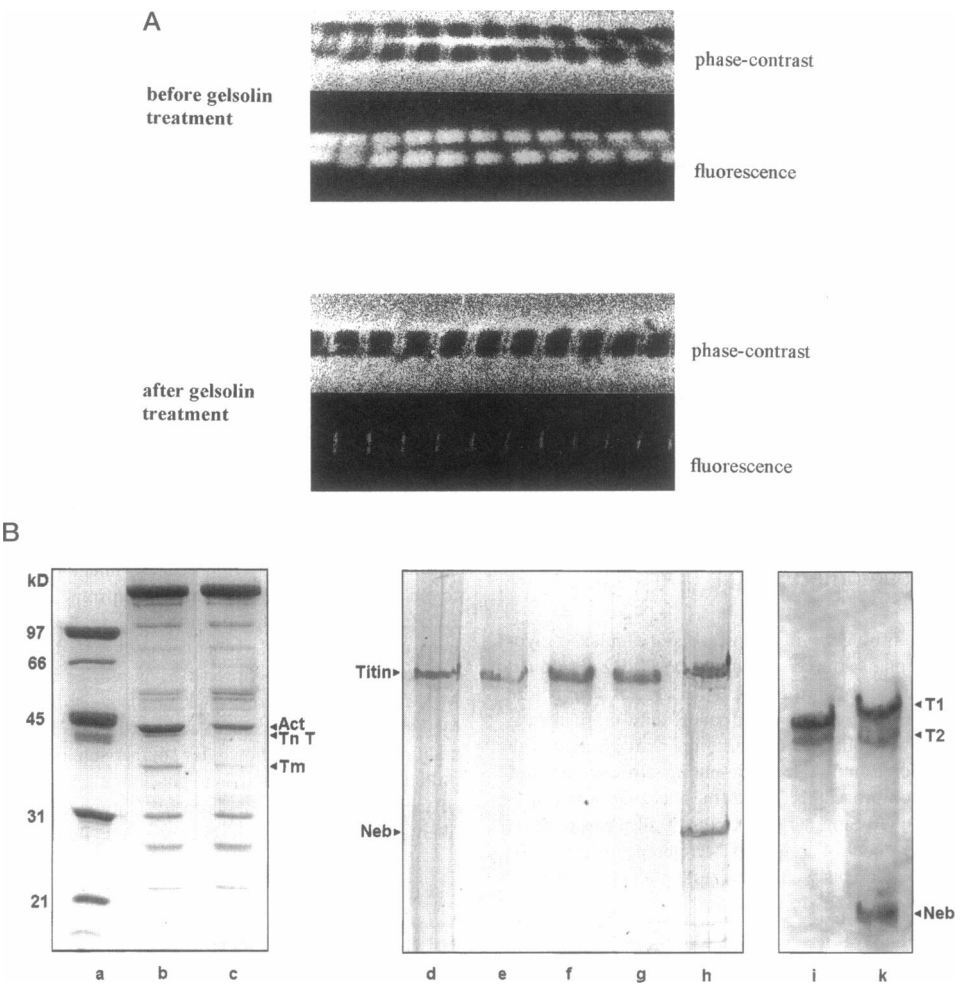

FIGURE 5 Testing myofibrils for quality of actin extraction and titin preservation. (*A*) Rhodamine-phalloidin staining on control (*top*) and actin-extracted (*bottom*) cardiac myofibrils. Actin appeared to be extracted by the gelsolin treatment, except for narrow regions localizing within the Z-discs. (*B*) 12% (*lanes a–c*) and 2% (*lanes d–k*) SDS-polyacrylamide gels prepared from suspensions of myofibrils. (*Lane a*) Molecular weight standard for *lanes b* and *c*. (*Lane b*) Control, relaxed, cardiac myofibrils. (*Lane c*) Cardiac myofibrils after 6-h gelsolin treatment (concentration, 0.2 mg/ml). (*Lane d*) Freshly prepared cardiac myofibrils. (*Lane e*) Freshly prepared cardiac myofibrils after 6-h gelsolin treatment (concentration, 0.2 mg/ml). (*Lane f*) One-week-long glycerinated cardiac myofibrils. (*Lane g*) One-week-long glycerinated cardiac myofibrils after 6-h gelsolin treatment (concentration, 0.2 mg/ml). (*Lane h*) For comparison: 3-week-long glycerinated skeletal myofibrils from rat *m. longissimus dorsi*. (*Lane i*) Two-week-long glycerinated cardiac myofibrils loaded in another 2% gel; more time was allowed for migration of proteins than in *lanes d–h*. (*Lane k*) Three-week-long glycerinated skeletal myofibrils (*m. longissimus dorsi*). Act, actin; TnT, troponin T; Tm, tropomyosin; Neb, nebulin; T1, a band that likely corresponds to native titin; T2, lower-molecular-weight titin band, which presumably appears because of proteolysis of native titin.

that actin, together with tropomyosin and troponin T, was largely extracted from myofibrils treated with 0.1–0.2 mg/ml gelsolin fragment (Fig. 5 *B*, *lanes a–c*). The residual actin was likely to represent the nonextractable Z-disc actin also seen in the fluorescence images. These results are in agreement with previous reports, which showed that Z-disc actin is resistent to severing by gelsolin fragment (Granzier and Wang, 1993) or gelsolin (Gonsior and Hinssen, 1995). In sum, fluorescence microscopy and SDS gels together revealed a uniform and high degree of actin extraction. Therefore it was unlikely that incomplete actin removal could be a cause of the observed variability in the amount of stiffness decrease.

Titin preservation

Another possible explanation for the variability in experimental results could be a certain degree of titin degradation, for instance, by gelsolin per se, which had been fragmented with the protease thermolysin. We checked for this possibility by analyzing 2% SDS-gels from both fresh and glycerinated myofibril suspensions, treated with 0.2 mg/ml gelsolin in relaxing solution for several hours. Fig. 5 *B* shows that neither in fresh (*lanes d* and *e*) nor in glycerinated (*lanes f* and *g*) cardiac specimens, was the appearance of the titin bands affected by gelsolin treatment. Such treatment thus does not impair titin preservation. Sometimes, however, a slight difference in the staining pattern of titin bands was apparent upon comparison of fresh and glycerinated myofibrils, such as widening of the titin band after glycerination (Fig. 5, *lanes f* and *g*) or the appearence of a second, lower titin band (T2; *lane i*), as has been found by others (e.g., Granzier and Irving, 1995). Thus a small degree of titin degradation during the glycerination process remains a possibility, despite the high amounts of protease inhibitors present in all solutions used. However, it seems clear that the upper titin band represents the native molecule (T1), because the T1 of skeletal myofibrils (Fig. 5 *B*, *lines h* and *k*) migrated a shorter distance than that of cardiac preparations, as expected for the higher-molecular-weight skeletal titins (Wang et al., 1991; Labeit and Kolmerer, 1995a). In conclusion, although titin degradation appeared to be very limited, it may have given rise to some variability in the magnitude of stiffness decrease upon actin extraction. Finally, a remaining possibility to be analyzed in the future is that some variability in experimental results may be caused by the presence of variable length isoforms of cardiac titin (Labeit and Kolmerer, 1995a) within a small myofibril bundle.

Actin extraction increases the extensibility of Z-disc-N1-line titin

We attempted to identify the sarcomeric elements responsible for the stiffness decrease with actin extraction by employing a number of different experimental techniques, such as biochemical assays, mechanical methods, and immunofluorescence microscopy. Previously it had been suggested that a possible site of actin-titin association could be the Z-disc-N1-line region, which is stiff under physiological conditions (Sebestyen et al., 1995; Trombitas et al., 1995). We therefore hypothesized that, if actin indeed associated with titin in that region, actin extraction might increase the compliance of the Z-disc-N1-line titin segment, thereby decreasing the overall stiffness of the sarcomere. Because such a stiffness change should go along with an increased extensibility of the Z-disc-N1-line titin region, we analyzed by fluorescence microscopy the stretch-dependent mobility of the T12 titin antibody epitope, known to localize within the sarcomere's N1-line (Fürst et al., 1988). To reproduce the experimental conditions of the stiffness measurements, we exposed the myofibrils to brief bursts of small-amplitude sinusoids, before carrying out the antibody labeling procedure. Fluorescence images were then recorded from both control and actin-extracted myofibrils.

The T12 antibody labeled two closely spaced stripes, one in each half-sarcomere near the Z-disc (Fig. 6 *A*). In control myofibrils at the shorter SLs, the two labeling sites were usually detected as a single, broad stripe, which was noticeably wider than the narrow stripe of residual actin that could be observed in the Z-disc region after gelsolin treatment and rhodamine-phalloidin labeling (cf. Fig. 5 *A*). In the control specimens, the titin epitopes remained almost stationary relative to the Z-disc over a SL range from 1.9 to 2.7 μm (Fig. 6, *A* and *B*, *left panels*; Fig. 6 *C*, *lower curve*). Only above that length did the epitope spacing increase more significantly. In contrast, the T12 epitope mobility was quite different after gelsolin treatment. Now the titin epitopes began to translate away from the Z-disc at much shorter SLs than in the intact myofibrils: the T12 epitope spacing already increased noticeably at 2.2 μm SL (Fig. 6, *A* and *B*, *right panels*; Fig. 6 *C*, *upper curve*). Accordingly, a summary of results (Fig. 6 *C*) shows that up to SLs of 3.3–3.4 μm, the slope of the T12 extension curve was steeper in the actin-depleted myofibrils than in the control specimens. It is noteworthy that the increase in extensibility of Z-disc-N1-line titin after actin removal was less obvious when we omitted the step of exposing the preparation to brief bursts of sinusoids before or during antibody labeling. In sum, these data indicate that actin extraction increases the extensibility of the Z-disc-N1-line titin region, which could then be responsible for the stiffness decrease.

In vitro assays reveal differences in actin-titin binding propensity along the sarcomere

To confirm the finding that sarcomere stiffness results in part from actin-titin binding, we carried out in vitro cosedimentation assays, in which multimodule recombinant titin fragments were tested for their ability to interact with F-actin. Fragment types from three distinctly different titin regions along the half-sarcomere were selected for the assay

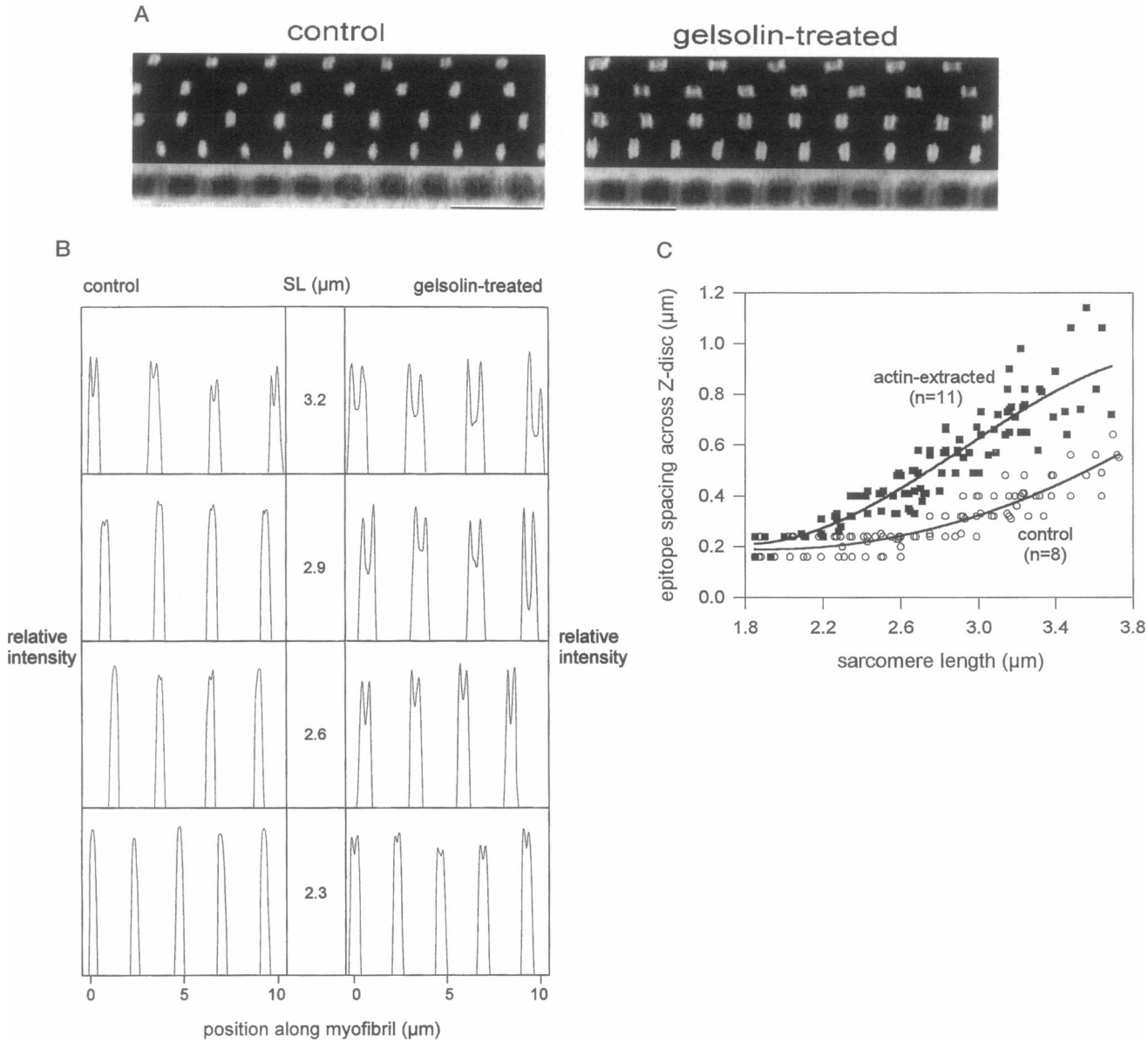

FIGURE 6 T12 titin antibody mobility before and after actin extraction. (*A*) Phase-contrast (*bottom image*) and fluorescence images of single cardiac myofibrils, labeled with the fluorophore-marked T12 antibody, and stretched to four different SLs (2.3, 2.6, 2.9, 3.2 μm, *from bottom to top*, respectively). Three images were recorded at a given SL and then superimposed to increase resolution. *Left images*: Myofibril before actin extraction; *right images*: a different myofibril after actin extraction. Scale bars, 5 μm. (*B*) Profile plots from selected regions along the myofibril axis, taken from the respective myofibrils shown in *A*. The intensities of four pixel lines were averaged. (*C*) Summary of SL-dependent T12 extension behavior before (○) and after (■) gelsolin treatment. For these experiments we used myofibrils prepared mostly from fresh muscle. In control myofibrils at the short SLs, at which the two T12 epitopes near the Z-disc appeared as one broad stripe (see *A*), we plotted stripe width, rather than epitope-epitope distance, across the Z-disc. The curves were obtained by third-order regression.

(Fig. 7): 1) the immunoglobulin (Ig)-like modules, Z10/I1, which are located just N-terminal from the T12 antibody epitope within the physiologically stiff N1-line region; 2) the whole cardiac PEVK segment and the tandem-Ig domain fragment, I27-I30, both from the elastic I-band titin section; and 3) the construct, A65/A68, which comprises four Ig/FN3 modules from the functionally stiff A-band titin portion (for titin domain designation, cf. Labeit and Kolmerer, 1995a).

When the first construct, Z10/I1, was assayed for F-actin binding, we detected the fragment in both the supernatant and the pellet, indicating actin-titin interaction (Fig. 8 *A*). The actin-binding propensity of the titin fragment was not particularly strong, as judged from the fact that saturation was not achieved up to the highest concentrations used (50 μM), but was considered significant. The almost identical molecular weights of the construct and actin made a quantitation of the Western blot fluorograms (Fig. 8 *A*, *bottom*)

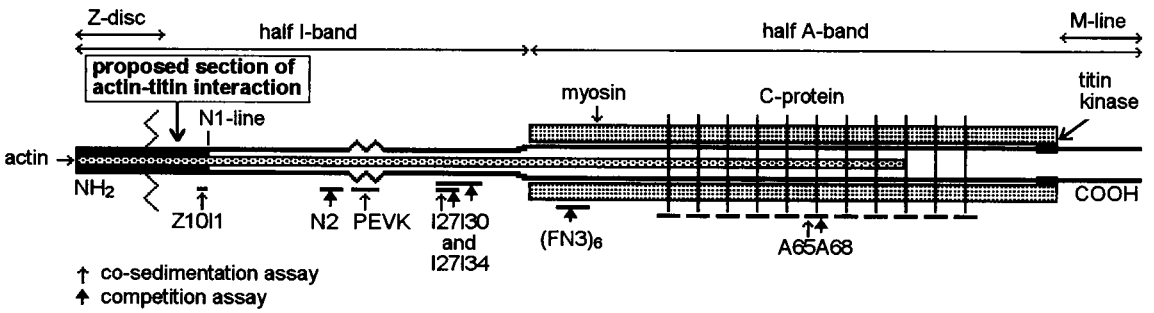

FIGURE 7 Layout of titin in the half-sarcomere. The proposed site of actin-titin interaction near the Z-disc is shown. The recombinant cardiac titin fragments used for the cosedimentation assays and the competition experiments, respectively, are indicated. Z10/I1: Two-Ig-domain fragment from the N1-line (also containing a large interdomain insertion); N2: four-Ig-domain fragment from the N2-titin segment (cf. Labeit and Kolmerer, 1995a); PEVK: recombinant segment comprising the whole cardiac titin sequence, rich in the amino acid residues proline (P), glutamate (E), valine (V), and lysine (K), flanked by the Ig domains, I18 and I20; I27/I30: four-domain fragment from the tandem-Ig region; I27/I34: eight-domain fragment from the tandem-Ig region; $(FN3)_6$: six-domain fragment consisting of a string of fibronectin-like domains at the distal end of the A-band (Bennett and Gautel, 1996); A65/A68: four-domain fragment, which is from the "super repeat" region of A-band titin (Labeit et al., 1992) and thus covers the C-zone of the half-sarcomere. Note that the half-sarcomere in this scheme is shown at a highly stretched length.

difficult. The apparent K_d of the construct, therefore, could not be assessed.

In contrast, neither fragment type from the elastic I-band titin region (cardiac PEVK segment; I27/I30) showed interaction with F-actin. Because of the similarity of results, only the gel and Western blot for I27/I30 are shown in Fig. 8 *B*. The fragments could consistently be detected in the supernatant, but were not detectable in the pellet, not even at concentrations of up to 50 μM, i.e., in 2.5-fold molar excess over actin. Similarly, the A-band titin fragment, A65/A68, also showed no association with actin (Fig. 8 *C*, *top*). This indicates that an interaction between these three titin constructs and F-actin is either too weak to be detectable with such small fragments or is completely absent. In summary, the results of the cosedimentation assays support the hypothesis that actin-titin association occurs in the Z-disc-N1-line region, but not along the remainder of the half-sarcomere.

Calcium dependence of F-actin-titin binding

We extended the cosedimentation assays to test whether the binding strength between actin and the titin fragments may be enhanced in the presence of calcium (for a rationale, cf. Kellermayer and Granzier, 1996). A representative result with the construct A65/A68 is shown in Fig. 8 *C* (*bottom*). Comparable amounts of fragment could be detected in the supernatant in both the presence and absence of calcium, whereas in the pellet, no fragment was detectable under either condition. Because no effect of calcium was found in any experiment, we conclude that the presence of calcium in these in vitro assays does not enhance actin-titin interaction.

Does competitive titin binding affect myofibril stiffness?

The issue of possible actin-titin interaction, apart from that near the Z-disc, was also investigated in the intact sarcomere in "titin competition" assays. In these assays, we measured the stiffness of cardiac myofibril bundles in relaxing solution and then tested the effect of increasing concentrations of recombinant titin fragments (size, 4–8 Ig/FN3 modules) on this stiffness. The fragment types used are indicated in Fig. 7 and Table 1; they included Ig/FN3 domains from both I-band and A-band titin. To test whether the recombinant fragments exhibit native structure, circular dichroism (CD) spectra in the far ultraviolet were recorded from one of the constructs (I27/I30) in physiological buffer (Fig. 9 *A*). The general appearance of the spectrum compares well with other spectra previously recorded from titin Ig domains (e.g., Politou et al., 1995) and indicates typical β-sheet structure. We took this result as indicative of a structural fold of the domains likely resembling that of the native modules. Finally, confirmation that the titin fragments are able to diffuse into the myofibrillar lattice was obtained from measurements with fluorescently labeled titin fragment (for an example, see Fig. 9 *B*).

We hypothesized that if sarcomere stiffness was based in part on interaction between titin and thin filaments outside the Z-disc comb, the recombinant titin fragments would compete with the respective segments on the native titin molecules for this interaction, which should result in some stiffness decrease. Such a decrease would be expected to be relatively small, given that we used four to eight domain-sized fragments, but it was considered to be detectable in the case of significant actin-titin interaction. Thereby we aimed to test whether the focal interaction between actin and titin filaments previously observed in vitro at physiological ionic strength (Kellermayer and Granzier, 1996) may translate into an effect on sarcomere stiffness.

We found that within the resolution capability of the system (maximum error $\pm 5\%$), none of the recombinant titin fragments affected cardiac myofibril stiffness. Data from a typical experiment are shown in Fig. 9 *C*, and a summary of results from all types of constructs used is

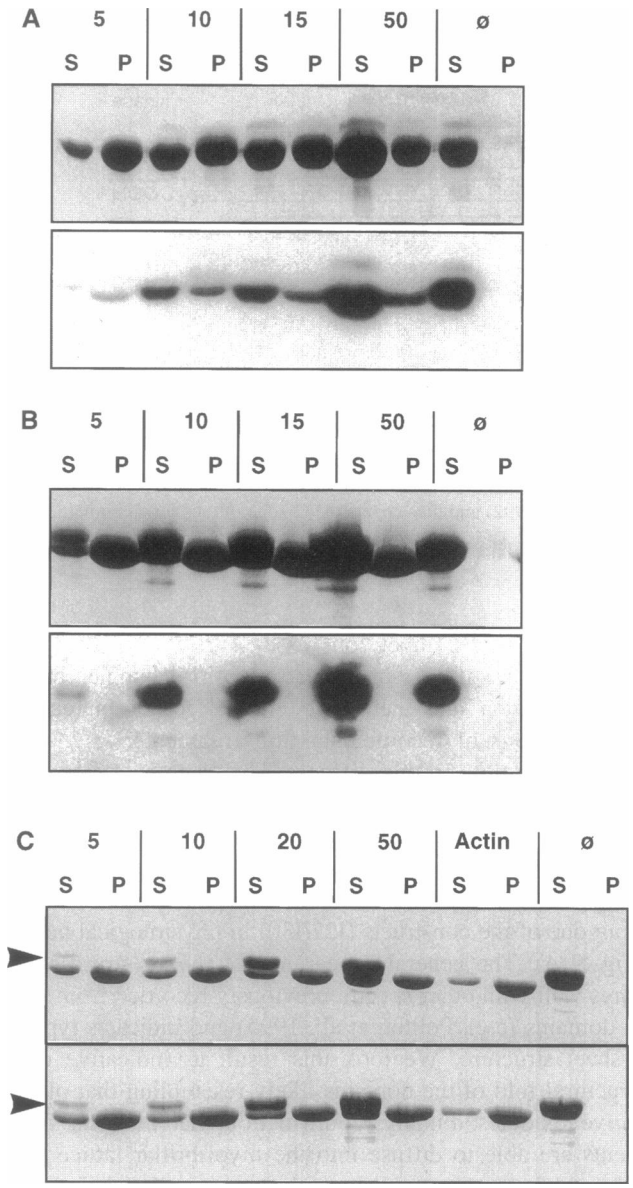

FIGURE 8 F-actin cosedimentation assays of recombinant multimodule fragments of titin in the presence of 1 mM EGTA. Fragment concentrations in μM are indicated above the panels. (*A*) F-actin cosedimentation assay of the Z-disc comb fragment, Z10/I1. Five microliters of the total reaction was loaded and electrophoresed as described in Materials and Methods. *Top:* Coomassie-stained SDS-gel; *bottom:* fluorograph of corresponding Western blot. Moderately strong binding of the fragment to F-actin is detected in the Western blot. (*B*) F-actin cosedimentation of the I-band fragment, I27/I30. Five microliters of the reaction was loaded. *Top:* Coomassie-stained SDS-gel; *bottom:* fluorograph of corresponding Western blot. The Western blot detects no protein in the pellets, indicating that the fragment does not bind to F-actin. (*C*) Cosedimentation assay of the C-zone fragment, A65/A68. The total reaction mix (2.5 μl) was loaded. Coomassie-stained SDS gels. *Top:* Assays in the presence of 1 mM EGTA; *bottom:* in the presence of 0.1 mM Ca^{2+}. The titin fragment is indicated by an arrowhead. No F-actin cosedimentation is detected, either in the presence or in the absence of Ca^{2+}. S, Supernatant; P, pellet; ø, control of fragment without actin; Actin: control with actin and no titin fragments.

presented in Table 1. In some experiments, we also applied a combination of two different recombinant fragment types, but again, no stiffness change was detectable. Although the possibility exists that the tendency of small titin fragments to bind actin is smaller and less competitive than that of titin, we found that even at high fragment concentrations of 10–15 mg/ml (I27/I30 and I27/I34), no stiffness change was apparent. These results suggest that outside the Z-disc-N1-line region, actin-titin interaction may not be a relevant factor in determining the mechanical properties of relaxed cardiac myofibrils.

DISCUSSION

Titin-actin interaction contributes to the elastic properties of relaxed cardiac myofibrils

It is well established that relaxed myofibrils from cardiac muscle are stiffer than those from skeletal muscle (Linke et al., 1994; Granzier and Irving, 1995). These differences can be largely explained by the expression of specific I-band titin sequences in different length isoforms in the two muscle types (Labeit and Kolmerer, 1995a; Linke et al., 1996b). On the other hand, the tissue-specific structure of I-band titin may not be a myofibril's only determinant of stiffness: researchers from several laboratories have recently proposed that in cardiac muscle, titin may bind to thin filament proteins (Funatsu et al., 1993; Jin, 1995; Li et al., 1995; Sebestyen et al., 1995; Trombitas et al., 1995), which could affect sarcomere stiffness. However, experimental proof in intact sarcomeres had not been obtained before this study. Therefore, the present work was initiated to investigate, in isolated cardiac myofibril preparations, whether the postulated titin-thin filament interaction may be of physiological relevance.

In the first place, we chose to study the issue of titin-thin filament association from a mechanical point of view, by measuring the stiffness of relaxed, isolated cardiac myofibrils both before and after selective removal of actin filaments. Previously the "passive" stiffness of cardiac myocytes has been measured after thin-filament extraction with high-salt solution (Brady and Farnsworth, 1986; Roos and Brady, 1989). However, this extraction procedure has low specificity and leaves plenty of room for ambiguity of interpretation. In contrast, gelsolin has been shown to effectively sever thin filaments, at least in cardiac myofibrils, with high specificity (Gonsior and Hinssen, 1995). In vivo, gelsolin requires the presence of calcium ions for its actin-severing activity. In this study we have used the purified N-terminal half of the gelsolin molecule, which fragments F-actin in the absence of calcium (Hellweg et al., 1993; cf. also Granzier and Wang, 1993). This property facilitated the investigation of actin-titin association under relaxing conditions.

Selective actin extraction was found to decrease the stiffness of relaxed cardiac myofibrils, on average by 57%, at SLs between 2.2 and 2.6 μm (Fig. 3). Because we con-

TABLE 1 Summary of results of competition experiments, in which the effect of application of recombinant titin fragments in relaxing solution on cardiac myofibril stiffness was tested

Type of recombinant titin fragment (no. of Ig/FN3 domains)	Range of concentrations applied (mg/ml)	Relative stiffness at maximum titin fragment concentration (%); 100% = control, relaxed stiffness; (mean ± SD)	No. of myofibrils
N2-titin segment (4)	0.04–1.0	101 ± 5	3
I27/I30 (4)	0.10–10.0	98 ± 5	7
I27/I34 (8)	0.50–15.0	97 ± 7	4
Fibronectin-like domains from A-band edge (6)	0.15–1.0	98 ± 6	4
A65/A68 $(4)_{11}$	0.12–0.8	101 ± 6	4
Mixture of N2-titin segment and I27/I30	Both fragment types: 0.07 –0.5	100 ± 4	3
Mixture of $(FN3)_6$ and A65/A68	Both fragment types: 0.05–0.6	102 ± 5	2

SL, 2.3–2.6 μm; sinusoidal oscillation frequency, 10–20 Hz.

firmed that this stiffness decrease was unrelated to the dissociation of actin-myosin interactions (Fig. 4), we concluded that it could hint at an interaction between actin and titin, which under physiological conditions may stiffen the sarcomere.

Comparison with skeletal muscle

The finding that cardiac myofibril stiffness decreases with actin extraction warrants comparison with previous work on skeletal muscle fibers, which has shown the effect of selective actin removal on passive force (Funatsu et al., 1990; Granzier and Wang, 1993). Although in the present study we mostly opted for measuring dynamic stiffness, rather than passive force, our results can be compared with the literature reports; we demonstrated that the force responses to low-frequency sinusoids measured here are unlikely to be related to elements other than the titin filaments and should principally reflect the passive force of the preparations (Figs. 1 and 2). Comparison of our results with the literature data on skeletal muscle shows obvious differences: in cardiac myofibrils, stiffness decreased greatly with actin removal (Fig. 3), whereas in rabbit psoas fibers, passive force remained almost constant (Funatsu et al., 1990) or even increased significantly (Granzier and Wang, 1993) after thin-filament extraction. These differences, although perhaps surprising, can potentially be explained by structural differences between skeletal and cardiac myofibrils.

Cardiac myofibrils do not contain nebulin, an ~800-kDa skeletal muscle-specific protein that runs along the sarcomeric thin filaments (Wang and Wright, 1988; Labeit and Kolmerer, 1995b), although they do contain nebulette (M_r 107 kDa), which flanks the Z-line in cardiac sarcomeres (Moncman and Wang, 1995). As for the skeletal muscle preparations, several studies have reported that thin filaments can resist extraction by gelsolin (Sanger et al., 1987; Huckriede et al., 1988; Gonsior and Hinssen, 1995). The latter authors also showed that the F-actin resistance to severing is conferred by nebulin. Clearly, the results of these studies are in conflict with those of the above-mentioned reports (Funatsu et al., 1990; Granzier and Wang, 1993), which had demonstrated actin removal by gelsolin or gelsolin fragment, also in skeletal muscle. In an attempt to explain this discrepancy, Gonsior and Hinssen (1995) suggested that actin extraction by gelsolin might become more effective after prolonged glycerination of the preparation, as in the study of Funatsu et al. (1990). Glycerination could destabilize the thin filaments (e.g., by the action of endogenous proteases or by weakening of hydrophobic protein interactions), so that they become more sensitive to gelsolin. Although this proposal does not sufficiently explain the results of Granzier and Wang (1993), who used fibers from freshly prepared skeletal muscle, it seems that actin is indeed more resistant to gelsolin in skeletal fibers than in cardiac myocytes. Whether nebulette (Moncman and Wang, 1995) could act to prevent the actin near the Z-disc from extraction by gelsolin in cardiac muscle is unclear at present. However, this study's results would indirectly argue against this possibility.

In addition, because of the close proximity of actin, nebulin, and titin filaments in skeletal muscle sarcomeres, it is possible that actin extraction promotes interaction between the stiff nebulin and titin. Consequently, the titin filaments may become less compliant than in the intact sarcomere, so that at a given SL, myofibril stiffness after actin removal is enhanced (cf. Granzier and Wang, 1993). In contrast, actin extraction in cardiac myofibrils should leave titin as the sole determinant of myofibril stiffness, perhaps with the exception of some intrasarcomeric intermediate filaments, whose stiffness contribution, however, is very small (Granzier and Irving, 1995). In conclusion, the presence of nebulin in skeletal, but not in cardiac, muscle might explain why gelsolin treatment has different effects on stiffness in the two muscle types.

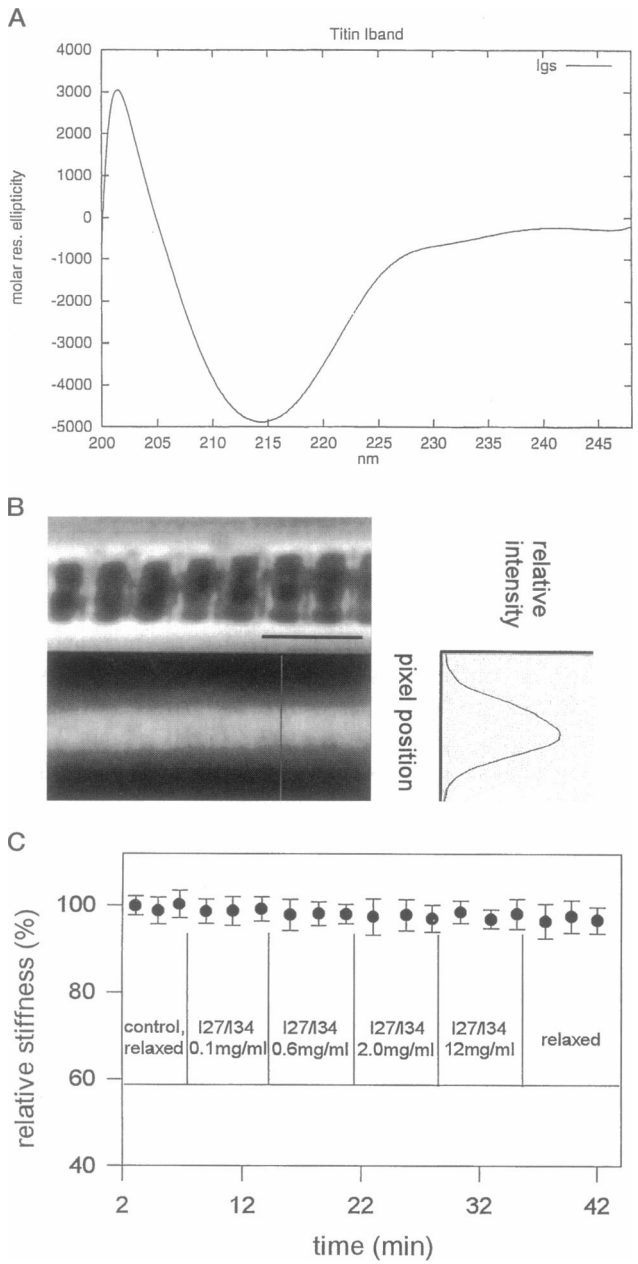

FIGURE 9 Titin competition experiments. (*A*) Normalized far-UV CD spectrum to test the folding of the four-module titin construct, I27/I30, in buffer. The spectrum was obtained at pH 7.1 and 25°C in rigor II buffer (see Myofibril preparation and solutions), which was used instead of relaxing buffer to reduce background noise due to the presence of ATP. Concentration of the construct was 4 μM, and the path length was 1 mm (cf. Politou et al., 1995). The single minimum around 214 nm is typical of a β-sheet structure. The general appearance compares well with other spectra of titin immunoglobulin domains (e.g., Politou et al., 1995). (*B*) Phase-contrast (*top*) and fluorescence (*bottom*) images of ~4-μm-thick myofibril bundle in relaxing buffer after a 20-min-long exposure to 0.8 mg/ml TRITC-labeled recombinant titin fragment, A65/A68 (for preparation, see Materials and Methods). The fluorescence image was recorded from a focal plane in the interior of the myofibril, shortly after quick washout of the titin fragment-containing solution. A65/A68 fragment is diffused both into I-bands and A-bands. Slight heterogeneity of fragment distribution is probably due to the presence of strong diffusion barriers such as Z-discs and M-lines. Horizontal scale bar: 5 μm; vertical bar: pixel line at which the profile plot shown to the right (representing fragment distribution perpendicular to the myofibril axis within the A-band) was recorded. (*C*) Stiffness of a ~4-μm-thick myofibril bundle in relaxing solution, to which the recombinant titin fragment, I27/I34 (cf. Fig. 7), was added in progressively increasing concentrations. Stiffness remained unchanged throughout the experiment. SL, 2.4 μm; sinusoidal oscillation frequency, 20 Hz. 100% stiffness refers to the stiffness during the first (control) measurement in relaxing solution.

Actin-titin interaction may not occur in the elastic I-band section or in the A-band

It had previously been suggested from the study of deep-etch replica electron micrographs of rabbit papillary muscle fibers that actin filaments may laterally associate with titin in the elastic I-band region (Funatsu et al., 1993). Because it is difficult to imagine, at the same time, both actin-titin association along major portions of the sarcomere and relative sliding of thin and thick filaments past one another during sarcomere shortening, the authors proposed that the interaction between actin and titin might occur transiently or weakly, such that myofibril shortening is not grossly impaired.

However, the present study does not (except for the Z-disc flanking regions) report evidence for actin-titin interaction along the cardiac muscle sarcomere. We demonstrated by in vitro cosedimentation assays that recombinant titin domains from the elastic I-band section (I27/I30; PEVK segment in I18/I20) and from the functionally stiff A-band region (A65/A68) do not associate with actin (Fig. 8, *B* and *C*). Likewise, in titin competition experiments, we found no mechanical evidence for actin-titin interaction in relaxed sarcomeres, either along the elastic I-band titin portion or in the A-band (Fig. 9 and Table 1). For obvious practical reasons, selected recombinant titin fragments were studied that do not cover the entire titin molecule. Therefore we cannot exclude the possibility that titin-thin filament interactions occur in regions not tested by us. Indeed, Jin (1995) has found that cloned rat cardiac titin fragments of one or two Ig/FN3 motifs can interact with actin in in vitro cosedimentation assays. Moreover, it was also shown that this two-domain-sized titin fragment slows down the velocity of actin filaments in an in vitro motility assay (Li et al., 1995). Although this finding has not yet been tested for its physiological relevance, it was suggested that actin-titin interaction might occur at some sites along the cardiac sarcomere, and that FN3 domains were making an important contribution to this interaction. Clearly, these results warrant comparison with those of the present study.

Sequence comparison of the fragment studied by Jin (1995) and Li et al. (1995) with the human cardiac titin sequence (Labeit and Kolmerer, 1995a) reveals that the construct is localized immediately N-terminal to the construct I48/I54 (six fibronectin domains) studied by us (94.2% identity to human cardiac titin peptide sequence from residues 7068 to 7274); it is localized within the characteristic Ig-FN3-FN3-Ig motif correlating with the myosin headgroup arrangement (Bennett and Gautel, 1996).

Moreover, it is also represented in the fragment A65/A68 investigated in this study. Because the binding of proteins via exposed hydrophobic patches is a common cause of nonspecific actin binding, the domain phasing of constructs used for cosedimentation assays must be chosen with great care. Our experiments were carried out with fragments whose boundaries were chosen based on the structural knowledge of titin domains (Politou et al., 1994; Improta et al., 1996). Furthermore, by analyzing CD spectra from constructs in physiological buffer, we showed evidence that tandem-Ig fragments used by us exhibit the expected β-sheet structural fold (Fig. 9 *A*). With those fragments—including the $(FN3)_6$ construct, located near the previously proposed site of actin-titin binding (Jin, 1995)—we found no effect on stiffness (Table 1) and no actin-binding propensity (Fig. 8, *B* and *C*, and unpublished observations). These data clearly demonstrate that neither for Ig-like titin domains nor for FN3 modules does interaction with actin appear to be a general feature.

In summary, if actin-titin interactions were present at all in the elastic I-band section and/or in the A-band of cardiac muscle sarcomeres, these interactions should be restricted to a few distinct sites. The recombinant titin fragments used in this study are representative of the main, characteristic, motif types of the titin molecule (i.e., tandem-Ig domains and PEVK-segment from the I-band, Ig/FN3-modules from the A-band). Considering that with these fragments, we found no evidence for actin-titin interaction outside the Z-disc comb, we favor the hypothesis that such an interaction does not occur in the intact sarcomere.

Actin-titin association stiffens the Z-disc-flanking regions of the sarcomere

Recent reports have discussed the possibility that titin-thin filament interaction may occur near the Z-disc (e.g., Sebestyen et al., 1995). An indication had been that the T12 titin antibody epitope, which is localized ~100 nm from the center of the Z-disc (at the N1-line), does not change its sarcomeric position during physiological amounts of stretch (Fürst et al., 1988; Trombitas et al., 1995). This could indicate either that titin has great intrinsic stiffness or that it associates with other proteins in the Z-disc-N1-line region. Evidence for actin-titin binding in that region is now presented in this study.

Moderately strong actin-titin binding propensity near the N1-line region was found in cosedimentation assays with F-actin and the recombinant titin fragment Z10/I1 (Fig. 8 *A*). This result is consistent with previous reports, which have shown interactions between native titin and actin in in vitro assays (Maruyama et al., 1987; Soteriou et al., 1993). Our result is then, to our knowledge, the first to show the potential of N-terminal titin domains to interact with actin. It should be remembered, however, that the actin binding to Z10/I1 is of rather low affinity (Fig. 8 *A*), which may imply that further molecular contacts exist between F-actin and other Z-disc-comb titin regions and/or that both proteins are involved in ternary complexes with other, unidentified ligands. Potential ligands could be, for example, tropomyosin and/or nebulette.

We also demonstrated that the in vitro actin-titin association is of functional relevance; in immunofluorescence measurements we found that the mobility of the T12 titin epitope upon sarcomere stretch is significantly increased after gelsolin treatment (Fig. 6). This indicates that actin extraction enhances the extensibility of the previously stiff Z-disc-N1-line titin region. Although this result does not necessarily imply actin-titin binding along the entire Z-disc-comb region, it clearly shows that interactions between the two filament systems contribute significantly to the functional stiffness of the Z-disc flanking titin segments in the intact sarcomere. Thus, just as the intrinsically elastic A-band region of titin is stiffened by its association with the myosin filament (Higuchi et al., 1992), titin is stiffened along its N-terminal region by association with the actin filament.

Can mobilization of Z-disc-flanking titin regions explain the magnitude of stiffness decrease?

To answer this question, one could argue as follows. If the nearly 60% stiffness decrease during actin extraction was brought about entirely by an increase in the contour length (ΔL_c) of the elastic titin segment (by mobilization of the Z-disc-N1-line titin region), one would expect ΔL_c to be equivalent to half the SL change, 0.5ΔSL (i.e., release), necessary to decrease the stiffness of the intact sarcomere by ~60%. Of course, this scenario requires that the elastic properties of both the physiologically extensible and the mobilized titin segment be similar.

Based on such reasoning, we can estimate from Figs. 2, 3 *B*, and 6 *C* of this study whether the amount of titin mobilization with gelsolin treatment is sufficient to explain a 60% stiffness decrease. We find that at an SL of ~2.6 μm, the Z-disc-N1-line titin regions of two half-sarcomeres combined lengthen by ~0.2 μm ($2\Delta L_c$ = 0.2 μm; Fig. 6 *C*), whereas stiffness decreases by almost 60% (Fig. 3 *B*). Likewise, during a 0.2-μm release of nonextracted myofibrils from an initial SL of 2.6 μm (ΔSL = 0.2 μm), stiffness also drops by ~60% (Fig. 2; also compare with figure 7 in Linke et al., 1996a). Hence the two above values for the stiffness change are the same within experimental error. In other words, ΔL_c is indeed equivalent to 0.5ΔSL. Therefore, mobilization of the Z-disc-flanking titin regions can explain the full magnitude of stiffness decrease with actin extraction.

The results obtained from measurements at both ends of the SL range studied warrant some comments. At SLs shortly above slack, we could not reliably determine the extent of titin segment length increase by immunofluorescence microscopy, because of the microscope's resolution limitations (Fig. 6 *C*). This issue should be reinvestigated in

the future, by using electron microscopy to increase resolution. In extremely stretched sarcomeres, the stiffness decrease during gelsolin treatment approached zero (Fig. 3 *B*), and the slope differences between the T12 extension curves disappeared (Fig. 6 *C*). It is clear from previous work that at SLs beyond the strain limit of cardiac myofibrils (~3 μm), both the previously stiff A-band titin portion and the Z-disc-N1-line titin segment become recruited into the elastic titin section (Trombitas et al., 1995; Linke et al., 1996a). Thus disintegration of the sarcomeric cytoskeleton at those extreme lengths may explain the lack of significant stiffness decrease with actin extraction above the "yield point."

An important issue is whether the molecular architecture of the Z-disc-N1-line titin region can potentially allow extensions on the order of those observed. Rhodamine-phalloidin fluorescence measurements have revealed that gelsolin treatment leaves a narrow strip of residual actin in the Z-disc (Fig. 5 *A*). Therefore, it is likely that not all titin domains between the center of the Z-disc and the N1-line become mobilized. In agreement with this proposal, a recent study of the N-terminal titin region of chicken breast muscle has shown that only approximately half the titin sequence previously assigned to the Z-disc (Labeit and Kolmerer, 1995a) is actually involved in Z-disc binding (Yajima et al., 1996). Also in cardiac muscle, the Z-disc titin region ends with domain Z4, as judged by immunoelectron microscopy (Gautel et al., 1996a). Thus N-terminal to the T12 epitope, there are approximately nine Ig domains and six unique sequence insertions (together comprising ~1100 amino acid residues), which do not yet enter the Z-disc but are stiff in the intact sarcomere. We suggest that these sequences make up the titin segment that becomes elastic upon actin extraction (see Fig. 7). Thus, with the assumption that this segment's maximum extension capacity is similar to that of cardiac I-band titin (maximum extension factor 8–10; Trombitas et al., 1995; Linke et al., 1996a), the observed amount of Z-disc-N1-line titin lengthening during actin extraction can readily be explained by mobilization of the previously stiff, Z-disc-flanking titin sequences.

CONCLUSION

In this study we have investigated in detail the issue of actin-titin interaction in relaxed cardiac myofibrils. Two conclusions seem especially noteworthy. First we could demonstrate that actin-titin interaction occurs in the Z-disc-comb region of the sarcomere, thereby providing a stiff anchorage for the elastic titin segment and making an important contribution to sarcomeric integrity at the high resting tension in cardiac muscle. Second, by screening for actin-titin interactions from the Z-disc to the A-band, we could exclude the possibility that binding to actin is a general feature of the titin molecule. Thus titin may not impair the relative sliding of thick and thin filaments past one another when the sarcomere changes length.

We are greatly indebted to Annalisa Pastore for help with the CD spectra and continuous support and to Michael Way for critical discussion of actin cosedimentation results. The authors are grateful to Dieter O. Fürst and Sonia Banuelos for kindly supplying the T12 antibody and the G-actin, respectively, and to Joseph Chalovich for letting us use the caldesmon prepared in his laboratory. We also thank Reinhold Wojciechowski and Claudia Liebetrau for expert technical assistance.

We gratefully acknowledge the financial support of the Deutsche Forschungsgemeinschaft (SFB 320 Rü; Li 690/2-1; Ga 405/3-1).

REFERENCES

Bartoo, M. L., V. I. Popov, L. A. Fearn, and G. H. Pollack. 1993. Active tension generation in isolated skeletal myofibrils. *J. Muscle Res. Cell Motil.* 14:498–510.

Bennett, P. M., and M. Gautel. 1996. Titin domain patterns correlate with the axial disposition of myosin at the end of the thick filament. *J. Mol. Biol.* 259:896–903.

Brady, A. J. 1968. Active state in cardiac muscle. *Physiol. Rev.* 48: 570–600.

Brady, A. J. 1991. Mechanical properties of isolated cardiac myocytes. *Physiol. Rev.* 71:413–428.

Brady, A. J., and S. P. Farnsworth. 1986. Cardiac myocyte stiffness following extraction with detergent and high salt solutions. *Am. J. Physiol.* 250:H932–H943.

Brenner, B., J. M. Chalovich, L. E. Greene, E. Eisenberg, and M. Schoenberg. 1986. Stiffness of skinned rabbit psoas fibers in MgATP and $MgPP_i$ solution. *Biophys. J.* 50:685–691.

Brinkmann, U., R. Mattes, and P. Buckel. 1989. High-level expression of recombinant genes in *Escherichia coli* is dependent on the availability of the dnaY gene product. *Gene.* 85:109–114.

Brotto, M. A. P., R. T. H. Fogaça, T. L. Creazzo, R. E. Godt, and T. M. Nosek. 1995. The effect of 2,3-butanedione 2-monoxime (BDM) on ventricular trabeculae from the avian heart. *J. Muscle Res. Cell Motil.* 16:1–10.

Chalovich, J. M., L. C. Yu, and B. Brenner. 1991. Involvement of weak binding cross-bridges in force production in muscle [news]. *J. Muscle Res. Cell Motil.* 12(6):503–506.

Fabiato, A., and F. Fabiato. 1976. Dependence of calcium release, tension generation and restoring forces on sarcomere length in skinned cardiac cells. *Eur. J. Cardiol.* 4:13–27.

Fabiato, A., and F. Fabiato. 1979. Calculator programs for computing the composition of the solutions containing multiple metals and ligands used for experiments in skinned muscle cells. *J. Physiol. (Lond.).* 75: 463–505.

Fearn, L. A., M. L. Bartoo, J. A. Myers, and G. H. Pollack. 1993. An optical fiber transducer for single myofibril force measurement. *IEEE Trans. Biomed. Eng.* 40:1127–1132.

Freiburg, A., and M. Gautel. 1996. A molecular map of the interactions of titin and myosin-binding protein C: implications for sarcomeric assembly in familial hypertrophic cardiomyopathy. *Eur. J. Biochem.* 235: 317–323.

Friedman, A. L., and Y. E. Goldman. 1996. Mechanical characterization of skeletal muscle myofibrils. *Biophys. J.* 71:2774–2785.

Funatsu, T., H. Higuchi, and S. Ishiwata. 1990. Elastic filaments in skeletal muscle revealed by selective removal of thin filaments with plasma gelsolin. *J. Cell Biol.* 110:53–62.

Funatsu, T., E. Kono, H. Higuchi, S. Kimura, S. Ishiwata, T. Yoshioka, K. Maruyama, and S. Tsukita. 1993. Elastic filaments in situ in cardiac muscle: deep-etch replica analysis in combination with selective removal of actin and myosin filaments. *J. Cell Biol.* 120:711–724.

Fürst, D. O., M. Osborn, R. Nave, and K. Weber. 1988. The organization of titin filaments in the half-sarcomere revealed by monoclonal antibodies in immunoelectron microscopy: a map of ten nonrepetitive epitopes starting at the Z-line extends close to the M-line. *J. Cell Biol.* 106: 1563–1572.

Gautel, M., D. Goulding, B. Bullard, K. Weber, and D. O. Fürst. 1996a. The central Z-disk region of titin is assembled from a novel repeat expressed in variable copy numbers. *J. Cell Sci.* 109:2747–2754.

Gautel, M., E. Lehtonen, and F. Pietruschka. 1996b. Assembly of the cardiac I-band region of titin/connectin: expression of the cardiac-specific regions and their relation to the elastic segments. *J. Muscle Res. Cell Motil.* 17:449–461.

Goa, I. 1953. A micro-biuret method for protein determination. *Scand. J. Clin. Lab. Invest.* 5:218–222.

Gonsior, S., and H. Hinssen. 1995. Exogenous gelsolin binds to sarcomeric thin filaments without severing. *Cell Motil. Cytoskeleton.* 31:196–206.

Granzier, H., M. Helmes, and K. Trombitas. 1996. Nonuniform elasticity of titin in cardiac myocytes: a study using immunoelectron microscopy and cellular mechanics. *Biophys. J.* 70:430–442.

Granzier, H. L., and T. C. Irving. 1995. Passive tension in cardiac muscle: contribution of collagen, titin, microtubules, and intermediate filaments. *Biophys. J.* 68:1027–1044.

Granzier, H. L., and K. Wang. 1993. Passive tension and stiffness of vertebrate skeletal and insect flight muscles: the contribution of weak cross-bridges and elastic filaments. *Biophys. J.* 65:2141–2159.

Harlow, E., and P. Lane. 1988. Labelling antibodies. *In* Antibodies: A Laboratory Manual. Cold Spring Harbor Laboratory, Cold Spring Harbor, NY. 319–358.

Hellweg, T., H. Hinssen, and W. Eimer. 1993. The Ca^{2+}-induced conformational change of gelsolin is located in the carboxy-terminal half of the molecule. *Biophys. J.* 65:799–805.

Higuchi, H., T. Suzuki, S. Kimura, T. Yoshioka, K. Maruyama, and Y. Umazume. 1992. Localization and elasticity of connectin (titin) filaments in skinned frog muscle fibres subjected to partial depolymerization of thick filaments. *J. Muscle Res. Cell Motil.* 13:285–294.

Hinssen, H., J. V. Small, and A. Sobieszek. 1984. A Ca^{2+}-dependent actin modulator from vertebrate smooth muscle. *FEBS Lett.* 166:90–95.

Horowits, R. 1992. Passive force generation and titin isoforms in mammalian skeletal muscle. *Biophys. J.* 61:392–398.

Horowits, R., E. S. Kempner, M. E. Bisher, and R. J. Podolski. 1986. A physiological role for titin and nebulin in skeletal muscle. *Nature.* 323:160–164.

Huckriede, A., H. Hinssen, B. M. Jockusch, and E. Lazarides. 1988. Gelsolin sensitivity of microfilaments as a marker for muscle differentiation. *Eur. J. Cell Biol.* 46:506–512.

Improta, S., A. Politou, and A. Pastore. 1996. Immunoglobulin-like modules from I-band titin: extensible components of muscle elasticity. *Structure.* 4:323–337.

Itoh, Y., T. Suzuki, S. Kimura, K. Ohashi, H. Higuchi, H. Sawada, T. Shimizu, M. Shibata, and K. Maruyama. 1988. Extensible and less-extensible domains of connectin filaments in stretched vertebrate skeletal muscle as detected by immunofluorescence and immunoelectron microscopy using monoclonal antibodies. *J. Biochem. (Tokyo).* 104: 504–508.

Jin, J.-P. 1995. Cloned rat cardiac titin class I and class II motifs. *J. Biol. Chem.* 270(12):6908–6916.

Kellermayer, M. S., and H. L. Granzier. 1996. Calcium-dependent inhibition of in vitro thin-filament motility by native titin. *FEBS Lett.* 380(3): 281–286.

Kraft, T., J. M. Chalovich, L. C. Yu, and B. Brenner. 1995. Parallel inhibition of active force and relaxed fiber stiffness by caldesmon fragments at physiological ionic strength and temperature conditions: additional evidence that weak cross-bridge binding to actin is an essential intermediate for force generation. *Biophys. J.* 68:2404–2418.

Labeit, S., M. Gautel, A. Lakey, and J. Trinick. 1992. Towards a molecular understanding of titin. *EMBO J.* 11:1711–1716.

Labeit, S., and B. Kolmerer. 1995a. Titins, giant proteins in charge of muscle ultrastructure and elasticity. *Science.* 270:293–296.

Labeit, S., and B. Kolmerer. 1995b. The complete primary structure of human nebulin and its correlation to muscle structure. *J. Mol. Biol.* 248:308–315.

Labeit, S., B. Kolmerer, and W. A. Linke. 1997. The giant protein titin. Emerging roles in physiology and pathophysiology. *Circ. Res.* 80: 290–294.

Laemmli, U. K. 1970. Cleavage of structural proteins during the assembly of the head of bacteriophage T4. *Nature.* 227:680–685.

Li, Q., J.-P. Jin, and H. Granzier. 1995. The effect of genetically expressed cardiac titin fragments on in vitro actin motility. *Biophys. J.* 69: 1508–1518.

Linke, W. A., M. L. Bartoo, M. Ivemeyer, and G. H. Pollack. 1996a. Limits of titin extension in single cardiac myofibrils. *J. Muscle Res. Cell Motil.* 17:425–438.

Linke, W. A., M. L. Bartoo, and G. H. Pollack. 1993. Spontaneous sarcomeric oscillations at intermediate activation levels in single isolated cardiac myofibrils. *Circ. Res.* 3:724–734.

Linke, W. A., M. Ivemeyer, N. Olivieri, B. Kolmerer, J. C. Rüegg, and S. Labeit. 1996b. Towards a molecular understanding of the elasticity of titin. *J. Mol. Biol.* 261:62–71.

Linke, W. A., V. I. Popov, and G. H. Pollack. 1994. Passive and active tension in single cardiac myofibrils. *Biophys. J.* 67:782–792.

Maruyama, K., D. H. Hu, T. Suzuki, and S. Kimura. 1987. Binding of actin filaments to connectin. *J. Biochem. (Tokyo).* 101(6):1339–1346.

Maruyama, K., S. Matsubara, R. Natori, Y. Nonomura, S. Kimura, K. Ohashi, F. Murakami, S. Handa, and G. Eguchi. 1977. Connectin, an elastic protein of muscle: characterization and function. *J. Biochem. (Tokyo).* 82:317–337.

Moncman, C. L., and K. Wang. 1995. Nebulette: a 107 kD nebulin-like protein in cardiac muscle. *Cell Motil. Cytoskeleton.* 32:205–225.

Politou, A., M. Gautel, C. Joseph, and A. Pastore. 1994. Immunoglobulin domains of titin are stabilized by N-terminal extension. *FEBS Lett.* 352:27–31.

Politou, A. S., D. J. Thomas, and A. Pastore. 1995. The folding and stability of titin immunoglobulin-like modules, with implications for the mechanism of elasticity. *Biophys. J.* 69:2601–2610.

Roos, K. P., and A. J. Brady. 1989. Stiffness and shortening changes in myofilament-extracted rat cardiac myocytes. *Am. J. Physiol.* 256: H539–H551.

Sanger, J. M., B. Mittal, A. Wegner, B. M. Jockusch, and J. W. Sanger. 1987. Differential response of stress fibers and myofibrils to gelsolin. *Eur. J. Cell Biol.* 43:421–428.

Sebestyen, M. G., J. A. Wolff, and M. L. Greaser. 1995. Characterization of a 5.4 kb cDNA fragment from the Z-line region of a rabbit cardiac titin reveals phosphorylation sites for proline-directed kinases. *J. Cell Sci.* 108:3029–3037.

Soteriou, A., M. Gamage, and J. Trinick. 1993. A survey of the interactions made by titin. *J. Cell Sci.* 104:119–123.

Tatsumi, R., and A. Hattori. 1995. Detection of giant myofibrillar proteins connectin and nebulin by electrophoresis in 2% polyacrylamide slab gels strengthened with agarose. *Anal. Biochem.* 224:28–31.

Trombitas, K., J.-P. Jin, and H. Granzier. 1995. The mechanically active domain of titin in cardiac muscle. *Circ. Res.*, 77:856–861.

Trombitas, K., and G. H. Pollack. 1993. Elastic properties of connecting filaments along the sarcomere. *Adv. Exp. Med. Biol.* 332:71–79.

Wang, K. 1996. Titin/connectin and nebulin: giant protein rulers of muscle structure and function. *Adv. Biophys.* 33:123–134.

Wang, K., R. McCarter, J. Wright, J. Beverly, and R. Ramirez-Mitchell. 1991. Regulation of skeletal muscle stiffness and elasticity by titin isoforms: a test of the segmental extension model of resting tension. *Proc. Natl. Acad. Sci. USA.* 88:7101–7105.

Wang, K., R. McCarter, R. Wright, J. Beverly, and R. Ramirez-Mitchell. 1993. Viscoelasticity of the sarcomere matrix of skeletal muscles. The titin-myosin composite filament is a dual-stage molecular spring. *Biophys. J.* 64:1161–1177.

Wang, K., J. McClure, and A. Tu. 1979. Titin: major myofibrillar component of striated muscle. *Proc. Natl. Acad. Sci. USA.* 76:3698–3702.

Wang, K., and J. Wright. 1988. Architecture of the sarcomere matrix of skeletal muscle: immunoelectron microscopic evidence that suggests a set of parallel inextensible nebulin filaments anchored at the Z line. *J. Cell Biol.* 107:2199–2212.

Yajima, H., H. Ohtsuka, Y. Kawamura, H. Kume, T. Murayama, H. Abe, S. Kimura, and K. Maruyama. 1996. A 11.5-kb 5′-terminal cDNA sequence of chicken breast muscle connectin/titin reveals its Z line binding region. *Biochem. Biophys. Res. Commun.* 223:160–164.